Conformational Analysis of Indole Alkaloids Corynantheine and Dihydrocorynantheine by Dynamic ^{1}H NMR Spectroscopy and Computational Methods: Steric Effects of Ethyl vs Vinyl Group

Dan Stærk, Per-Ola Norrby, and Jerzy W. Jaroszewski*

Department of Medicinal Chemistry, The Royal Danish School of Pharmacy, Universitetsparken 2, DK-2100 Copenhagen, Denmark

jj@dfh.dk

Received June 29, 2000

^{1}H NMR (400 MHz) spectra of the indole alkaloid dihydrocorynantheine recorded at room temperature show the presence of two conformers near coalescence. Low temperature ^{1}H NMR allowed characterization of the conformational equilibrium, which involves rotation of the 3-methoxypropenoate side chain. Line-shape analysis yielded enthalpy of activation $\Delta H^\ddagger = 71 \pm 6$ kJ/mol, and entropy of activation $\Delta S^\ddagger = 33 \pm 6$ J/mol·K. The major and minor conformation contains the methyl ether group above and below the plane of the ring, respectively, as determined by low-temperature NOESY spectra, with free energy difference $\Delta G° = 1.1$ kJ/mol at −40 °C. In contrast to dihydrocorynantheine, the corresponding rotamers of corynantheine are in the fast exchange limit at room temperature. The activation parameters determined for corynantheine were $\Delta H^\ddagger = 60 \pm 6$ kJ/mol and $\Delta S^\ddagger = 24 \pm 6$ J/mol·K, with $\Delta G° = 1.3$ kJ/mol at −45 °C. The difference in the exchange rates of the rotamers of corynantheine and dihydrocorynantheine (respectively, 350 s^{-1} and 9 s^{-1} at 0 °C) reflects the difference in the steric bulk of the vinyl and the ethyl group. The conformational equilibria involving the side chain rotation as well as inversion of the bridgehead nitrogen in corynantheine and dihydrocorynantheine was studied by force-field (Amber* and MMFF) and ab initio (density-functional theory at the B3LYP/6-31G* level) computational methods, the results of which were in good agreement with the ^{1}H NMR data. However, the calculations identified the rotamers as essentially isoenergetic, the experimental energy differences being to small to be reproduced exactly by the theory. Comparison of density-functional and force-field calculations with experimental results identified Amber* as giving the most accurate results in the present case.

Introduction

The *Corynanthe*-type alkaloids dihydrocorynantheine (**1**) and corynantheine (**2**) are classical indole alkaloids isolated from Rubiaceous plants.[1−8] They have been a subject of extensive synthetic investigations.[7−15] Recently, **1** and **2** were shown to be potent inhibitors of *Leishmania major* promastigotes.[16] Closely related indole alkaloids exhibit antiviral[17] and analgesic activity.[18,19]

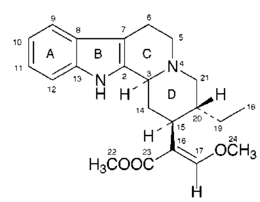

1

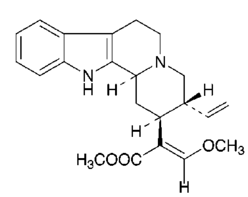

2

Although ^{13}C NMR spectra[14,16,20−22] of the *Corynanthe*-type alkaloids have been used extensively for structural

* To whom correspondence should be addressed. Fax + 45 3530 6040.

(1) Karrer, P.; Salomon, H. *Helv. Chim. Acta* **1926**, *9*, 1059.
(2) Janot, M.-M.; Goutarel, R. *C. R. Hebd. Seances Acad. Sci.* **1938**, *206*, 1183.
(3) Janot, M.-M.; Goutarel, R. *Bull. Soc. Chim. Fr.* **1951**, 588.
(4) Karrer, P.; Schwyzer, R.; Flam, A. *Helv. Chim. Acta* **1952**, *35*, 851.
(5) Goutarel, R.; Janot, M.-M.; Mirza, R.; Prelog, V. *Helv. Chim. Acta* **1953**, *36*, 337.
(6) Marion, L. *Alkaloids (Academic Press)* **1952**, *2*, 369.
(7) Saxton, J. E. *Alkaloids (Academic Press)* **1965**, *7*, 1.
(8) Manske, R. H. F. *Alkaloids (Academic Press)* **1965**, *8*, 693.
(9) Van Tamelen, E. E.; Hester, J. B., Jr. *J. Am. Chem. Soc.* **1959**, *81*, 3805.
(10) Van Tamelen, E. E.; Hester, J. B., Jr. *J. Am. Chem. Soc.* **1969**, *91*, 7342.
(11) Van Tamelen, E. E.; Wright, I. G. *J. Am. Chem. Soc.* **1969**, *91*, 7349.
(12) Szantay, C.; Barczai-Beke, M. *Chem. Ber.* **1969**, *102*, 3963.
(13) Barczai-Beke, M.; Dörnyei, G.; Toth, G.; Tamas, J.; Szantay, C. *Tetrahedron* **1976**, *32*, 1153.
(14) Szantay, C.; Blasko, G.; Honty, K.; Dörnyei, G. *Alkaloids (Academic Press)* **1986**, *27*, 131.
(15) Takayama, H.; Sakai, S.-I. *Alkaloids (Academic Press)* **1998**, *50*, 415.
(16) Stærk, D.; Lemmich, E.; Christensen, J.; Kharazmi, A.; Olsen, C. E.; Jaroszewski, J. W. *Planta Medica* **2000**, *66*, 531.
(17) Takayama, H.; Iimura, Y.; Kitayama, M.; Aimi, N.; Konno, K.; Inoue, H.; Fujiwara, M.; Mizuta, T.; Yokota, T.; Shigeta, S.; Tokushida, K.; Hanasaki, Y.; Katsuura, K. Bioorg. *Med. Chem. Lett.* **1997**, *7*, 3145.
(18) Yamamoto, L. T.; Horie, S.; Takayama.; H, Aimi.; N, Sakai, S.; Yano, S.; Shan, J.; Pang, P. K.; Ponglux, D.: Watanabe, K. *Gen. Pharmacol.* **1999**, *33*, 73.
(19) Watanabe, K.; Yano, S.; Horie, S.; Yamamoto, L. T. *Life Sci.* **1997**, *60*, 933.
(20) Wenkert, E.; Bindra, J. S.; Chang, C.-J.; Cochran, D. W.; Schell, F. M. *Acc. Chem. Res.* **1974**, *7*, 46.
(21) Koch, M. C.; Plat, M. M.; Preaux, N.; Gottlieb, H. E.; Hagaman, E. W.; Schell, F. M.; Wenkert, W. *J. Org. Chem.* **1975**, *40*, 2836.
(22) Wenkert, E.; Chang, C.-J.; Chawla, H. P. S.; Cochran, D. W.; Hagaman, E. W.; King, J. C.; Orito, K. *J. Am. Chem. Soc.* **1976**, *98*, 3645.

10.1021/jo000987n CCC: $20.00
Published on Web 03/13/2001

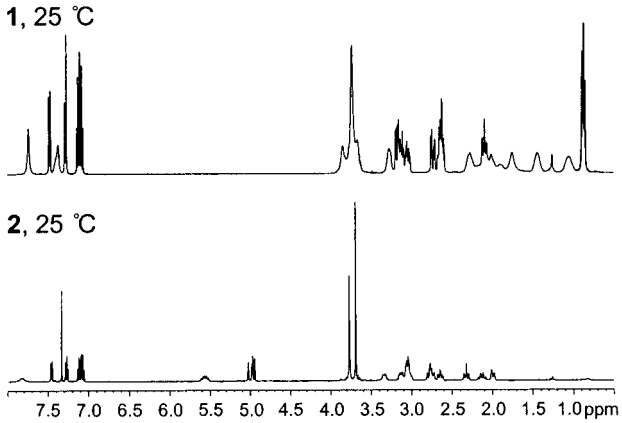

Figure 1. 400 MHz ^{1}H NMR spectra of **1** and **2** ($CDCl_3$, 25 °C).

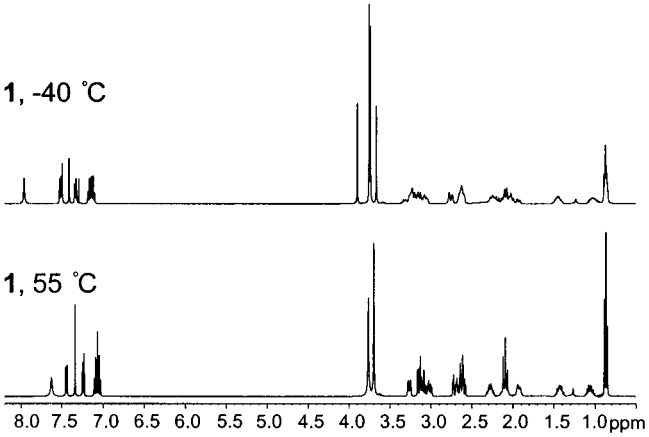

Figure 2. 400 MHz ^{1}H NMR spectra of **1** at −40 °C and 55 °C ($CDCl_3$).

correlations, information about their ^{1}H NMR data is scarce.[16] In this paper, we show that ^{1}H NMR spectra of *Corynanthe* alkaloids can be affected by dynamic processes. Conformational equilibria underlying the observed chemical exchange are characterized by variable-temperature NMR and computational methods.

Results and Discussion

^{1}H NMR spectra of dihydrocorynantheine (**1**) and corynantheine (**2**) recorded at room temperature exhibited pronounced differences (Figure 1). Thus, extensive line broadening of the aliphatic resonances, in particular of ring D and its side chains, was observed in the spectrum of **1**, whereas the unsaturated analogue **2** gave sharp lines at room temperature. Heating of the solution of **1** above 50 °C collapsed the resonances into a set of sharp signals, whereas cooling to −40 °C resulted in a spectrum of a mixture of two conformers in a ratio of 1:1.7 (Figure 2).

According to a Monte Carlo conformational search, compound **1** has two principal low-energy conformations, representing rotamers of the side chain attached to C(15). These conformations are characterized by the H(15)−C(15)−C(16)−C(17) torsion angle of about 180 and 0°, respectively (Figure 3). The two structures, in which the methyl ester group is either below (i.e., on the α-side) or above (on the β-side) the plane of the tetracyclic ring system, are hereinafter called conformation I and II,

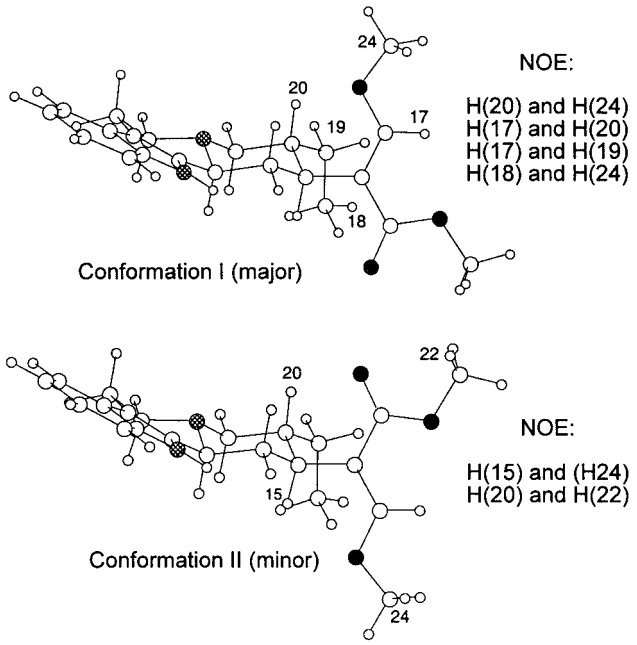

Figure 3. Amber*-optimized structures of low-energy conformations of **1**. Conformation I and II has the H(15)−C(15)−C(16)−C(17) torsion angle of 178.4° and −10.5°, respectively. Oxygen atoms are represented as black and nitrogen atoms as gray spheres.

respectively (Figure 3). In both conformations the quinolizidine system is trans-fused. Rotations about other single bonds in the side chains are expected to be fast on the NMR time scale within the temperature range examined.

NOESY spectra confirmed that the two conformations present in the solution of **1** at low temperature correspond to those shown in Figure 3. Thus, NOE from H(24) to H(18) and H(20) in the major and to H(15) in the minor conformation were observed. The NOE between H(18) and H(24) is due to the fast rotation of the ethyl group about the C(19)−C(20) bond. The olefinic proton H(17) showed NOE to H(19) and H(20) in the major but not in the minor conformation. On the other hand, the methyl ester protons H(22) showed correlation to H(20) in the minor but not in the major conformation. Therefore, the major conformation has the methyl ester group below and the methyl ether group above the ring plane, as in the conformation I (Figure 3). The population of the two conformers determined from the ^{1}H NMR spectra corresponds to a free energy difference of 1.1 kJ/mol at −40 °C. ^{1}H NMR data for the two conformations are collected in Table 1. In the major conformation, the olefinic hydrogen H(17) forms a doublet with $^4J_{15,17} \approx 0.5$ Hz (numeric value), whereas no coupling is observed in the minor conformation ($^4J_{15,17} \approx 0$ Hz). Since transoid allylic coupling constant depends markedly on the dihedral angle φ between the allylic C−H bond and the double bond, with $|^4J(\varphi = 180°)| > |^4J(\varphi = 0°)|$,[23] this agrees with the conclusion that the major conformation is conformation I.

As the energy difference between conformation I and II is very small, it is expected that the position of the equilibrium may not be reproduced exactly by the cal-

(23) Barfield, M.; Spear, R. J.; Sternhell, S. *Chem. Rev.* **1976**, *76*, 593.

Table 1. ^{1}H NMR Data (400 MHz, $CDCl_3$) for Conformers of *rac*-1 at Fast and Slow Exchange

	chemical shift, δ[a]		
proton	fast exchange (55 °C)	conformation I (−40 °C)	conformation II (−40 °C)[b]
1	7.63 (br s)	7.89 (br s)	7.87 (br s)
3	3.26 (d, $^3J_{3,14ax} = 11.6$)	3.26 (d, $^3J_{3,14ax} = 11.5$)	3.32 (d, $^3J_{3,14ax} = 11.5$)
5ax	2.61 (dt, $^2J_{5ax,5eq} = {}^3J_{5ax,6ax} =$ 10.6 Hz, $^3J_{5ax,6eq} = 4.3$)	2.63 (m)	
5eq	3.10 (m)	3.14 (m)	
6ax	3.02 (m)	3.06 (m)	
6eq	2.71 (m)	2.75 (m)	
9	7.44 (d, $^3J_{9,10} = 7.1$)	7.50 (d, $^3J_{9,10} = 7.4$)	
10	7.07 (dt, $^3J_{10,9} = {}^3J_{10,11} =$ 7.2, $^4J_{10,12} = 1.6$)	7.10 (dt, $^3J_{10,9} = {}^3J_{10,11} =$ 7.4, $^4J_{10,12} = 1.1$)	
11	7.11 (dt, $^3J_{11,10} = {}^3J_{11,12} =$ 7.2, $^4J_{11,9} = 1.6$)	7.15 (t, $^3J_{11,10} = {}^3J_{11,12} = 7.2$)	
12	7.24 (d, $^3J_{12,11} = 7.2$)	7.32 (d, $^3J_{12,11} = 7.4$)	7.31 (d, $^3J_{12,11} = 7.4$)
14ax	2.10 (q, $^3J_{14ax,3} = {}^3J_{14ax,15} =$ $^2J_{14ax,14eq} = 11.4$)	2.14 (m)	
14eq	1.92 (d, $^2J_{14eq,14ax} = 11.4$)	2.00 (d, $^2J_{14eq,14ax} = 12.4$)	1.91 (d, $^2J_{14eq,14ax} = 12.4$)
15	2.64(m)	2.63 (m)	
17	7.34 (s)	7.39 (d, $^4J_{17,15} = 0.5$)	7.46 (s)
18	0.87 (t, $^3J_{18,19} = 7.5$)	0.87 (t, $^3J_{18,19} = 7.3$)	0.86 (t, $^3J_{18,19} = 7.3$)
19A	1.43 (ddq, $^2J_{19A,19B} = 13.9$, $^3J_{19A,18} = 7.6$, $^3J_{19A,20} = 3.4$)	1.45 (m)	
19B	1.06 (dp, $^2J_{19A,19B} = 13.9$, $^3J_{19B,18} = 7.6$, $^3J_{19B,20} = 7.6$)	1.04 (m)	
20	2.28 (m)	2.30 (m)	2.24 (m)
21ax	2.09 (t, $^2J_{21ax,21eq} = {}^3J_{21ax,20} = 11.1$)	2.09 (m)	
21eq	3.14 (dd, $^2J_{21ax,21eq} = 11.1$, $^3J_{21eq,20} = 3.9$)	3.21 (m)	
22	3.69 (s)	3.75 (s)	3.66 (s)
24	3.76 (s)	3.74 (s)	3.88 (s)

[a] Coupling constants given as apparent splittings in Hz. [b]Only δ values different from those in conformation I are reported.

Table 2. Calculated Relative Energies of Principal Conformers of 1 and 2 and of the Corresponding Transition States in Vacuum and in Chloroform (kJ/mol)[a]

structure	1	2
conf. I, C/D trans	0[b,c] (0)	1.51[d,e] (0.70)
conf. II, C/D trans	1.45[b,c] (1.68)	0[d,e] (0)
transition state for bond rotation[f]	54.3 (53.8)	43.1 (42.8)
conf. I, C/D cis	4.45 (3.38)	3.06 (3.14)
conf. II, C/D cis	2.0 (2.61)	3.22 (4.60)
transition states for nitrogen inversion[g]	32.5 (33.8)	31.2 (31.6)
	33.0 (31.1)	31.1 (31.6)

[a] Relative energies in vacuo calculated using the Amber* force field, unless otherwise stated; values in chloroform (GB/SA solvation model) are given in parentheses. [b]With the MMFF force field, conformation II was favored by 2.8 kJ/mol (in vacuo). [c]Ab initio calculations at the B3LYP/6-31G* level favor conformation II by 0.1 kcal/mol (in vacuo). [d]With the MMFF force field, conformation I was favored by 7.7 kJ/mol (in vacuo). [e]At the B3LYP/6-31G* level, the energy difference between conformation I and II is 0.0 kJ/mol (in vacuo). [f]Energy (relative to global mimimum) of the lowest-energy transition state for C(15)−C(16) bond rotation. [g] Energies (relative to global minimum) of two transition states available for inversion of N(4).

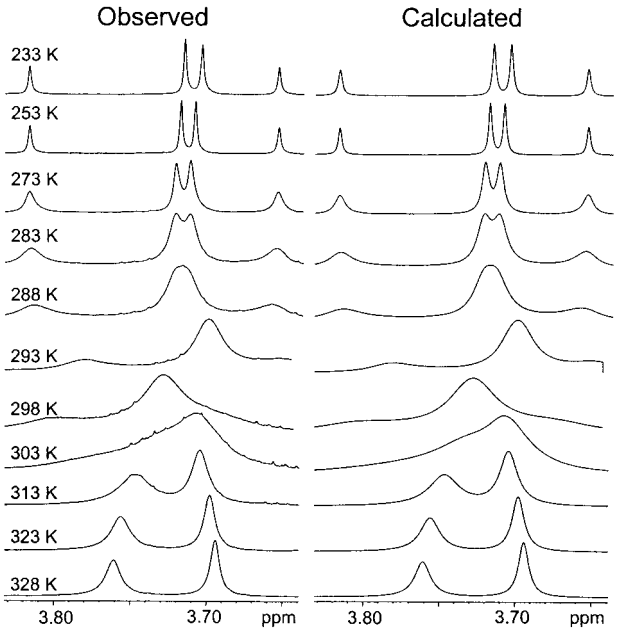

Figure 4. Observed (left) and calculated (right) 400 MHz ^{1}H NMR spectra ($CDCl_3$) of the methoxy group region of **1**.

culations. Thus, while Amber* force field correctly identified the major conformer (in a vacuum as well as in chloroform) with a very good agreement with the experimental energy difference, MMFF erroneously predicted the conformer II to be favored by 2.8 kJ/mol (Table 2). However, this error is only slightly larger than what is generally observed for conformational energies of small molecules.[24] Optimization of the energy of the two conformations by the density functional ab initio theory showed that the gas phase conformations are essentially isoenergetic, with the energy difference of 0.1 kJ/mol in favor of conformation II (Table 2). Thus, all computational methods agree that the two conformations are very close in energy, but the accuracy of the calculations is indeed insufficient to reproduce the experimental findings exactly.

Kinetics of the exchange between the two conformers of **1** was studied by full line-shape analysis of the methoxy group resonances in the temperature range from −40 to +55 °C (Figure 4). Eyring plot of the determined exchange rates at different temperatures yielded activation parameters $\Delta H^{\ddagger} = 71 \pm 6$ kJ/mol and $\Delta S^{\ddagger} = 33 \pm 6$ J/mol·K. A calculated energy profile for the rotation of the C(15)−C(16) bond is shown in Figure 5. It is appar-

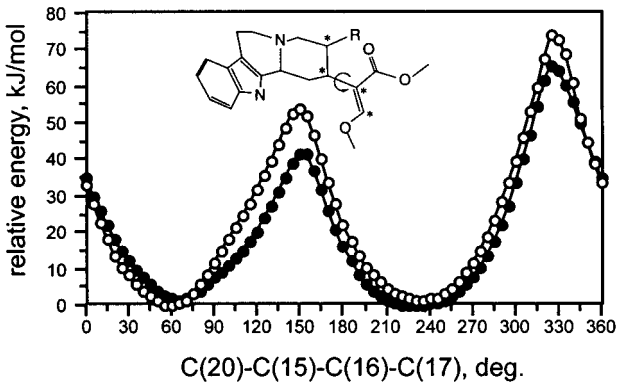

Figure 5. Calculated energy profiles (Amber*) for rotation of the C(15)−C(16) bond in **1** (open circles) and **2** (filled circles).

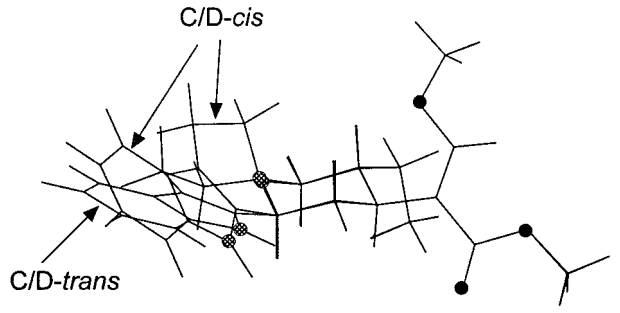

Figure 6. Superimposition of the minimum-energy conformation of **1** with a conformation with inverted N(4). Oxygen atoms are represented as black and nitrogen atoms as gray spheres.

ent, that only one pathway for the rotation, involving an eclipsing of C(14) with C(17), is energetically feasible. The calculated energy barrier for this transition is about 54 kJ/mol (Table 2), in reasonable agreement with the experimental value.

In addition to the rotation of the C(15)−C(16) bond, the calculations have disclosed a faster, but still relatively slow, conformational process, i.e., an inversion of the nitrogen N(4) to give a cis fusion of the rings C and D. A calculated energy barrier for this process, which can take place via one of two energetically equivalent transition states, is about 33 kJ/mol (Table 2). Since the energy barrier for the ring inversion is more than 20 kJ/mol lower than that for the bond rotation, the ring inversion is in the fast exchange region during observation of the bond rotation process (Figure 4). The conformation with cis C/D-fusion is predicted to be only slightly less stable (<5 kJ/mol) than trans-fused conformation, which is as expected a much smaller difference than for unsubstituted quinolizidine.[25,26] The nitrogen inversion causes no appreciable change of the geometry of ring D (Figure 6) and is therefore not expected to affect the NMR parameters of this part of the molecule to any significant extent.

For the unsaturated analogue **2**, the energy barrier for rotation of the C(15)−C(16) bond was calculated to be about 11 kJ/mol lower than for **1** (Amber*, Table 2). Accordingly, a 400 MHz ^{1}H NMR spectrum of **2** did not show any exchange broadening at room temperature

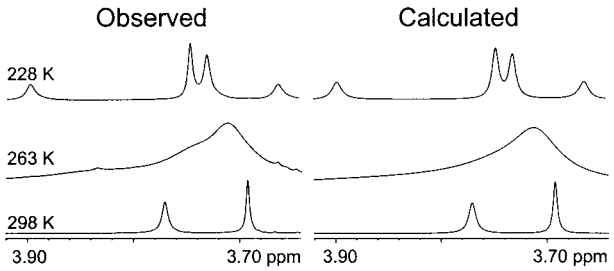

Figure 7. Observed (left) and calculated (right) 400 MHz ^{1}H NMR spectra ($CDCl_3$) of the methoxy group region of **2** at −45 °C, −10 °C, and 25 °C.

(Figure 1), but low-temperature spectra disclosed the presence of two rotamers analogous to those observed with **1** (Figure 7). The ratio between the rotamers of **2** was 1:2 at −45 °C, corresponding to free energy difference of 1.3 kJ/mol, very similar to that determined for **1**. In the case of **2**, the barrier for nitrogen N(4) inversion was predicted to be only about 10 kJ/mol lower than that for the rotational process (Table 2). The low barrier for the C(15)−C(16) bond rotation together with the presence of a four-site exchange system hampered unambiguous assignment of structure of the major and minor rotamer from low-temperature NOESY spectra. However, from the similarity of the chemical shifts of methoxy resonances of **1** (Figure 4) and **2** (Figure 7) at low temperature, it is concluded that the same conformation (conformation I) predominates in each case, in disagreement with the force-field results (Table 2). Density-functional theory showed the two conformations to be exactly isoenergetic (Table 2). Of the two force-fields used, Amber* and MMFF, only the former gave results with reasonable agreement with experimental and ab initio results and is the method of choice in the present case.

The exchange rate constants determined for **2** gave a linear Eyring plot in the temperature range from −35 °C to +5 °C, affording $\Delta H^{\ddagger} = 60 \pm 6$ kJ/mol and $\Delta S^{\ddagger} = 24 \pm 6$ J/mol·K. There is thus an excellent agreement between the calculated (Amber* in vacuo as well as in chloroform) and experimental difference of the energy barrier for the C(15)−C(16) bond rotation in **1** and **2** of 10 kJ/mol (Table 2).

In conclusion, the present work characterizes the conformational equilibria of **1** and **2** in terms of structure of the conformers and energy differences, as well as the activation parameters for conformational exchange. The two alkaloids exhibit marked differences in rotational energy barriers due to different steric effects of the neighboring vinyl and ethyl group. The explanation of dynamic processes influencing ^{1}H NMR spectra described in this work is of practical interest to those working with this type of indole alkaloids. Moreover, the equilibria described constitute an interesting example for testing computational methods for their ability to reproduce fine energy differences in medium-size molecules.

Experimental Section

The alkaloids **1** and **2** were isolated from bark of *Corynanthe pachyceras*.[16] A synthetic[13] sample of *rac*-**1** was a gift from Dr. I. Toth, School of Pharmacy, University of Queensland, Australia. All samples were purified by reversed phase HPLC (16 × 250 mm column of LiChrospher-100, RP18, eluted with 70% methanol in 0.01 M aqueous ammonium acetate adjusted to pH 8.04).[16]

(24) Gundertofte, K.; Liljefors, T.; Norrby, P.-O.; Pettersson, I. *J. Comput. Chem.* **1996**, *17*, 429.
(25) Moynehan, T. M.; Schofield, K.; Jones, R. A. Y.; Katritzky, A. R. *J. Chem. Soc.* **1962**, 2637.
(26) Johnson, C. D.; Jones, R. A. Y.; Katritzky, A. R.; Palmer, C. R.; Schofield, K.; Wells, R. J. *J. Chem. Soc.* **1965**, 6797.

NMR spectra were recorded at 400.13 MHz for ^{1}H and at 100.62 MHz for ^{13}C, using 27 mM solutions in $CDCl_3$. NOESY spectra were acquired using mixing times of 200−800 ms. Standard library pulse sequences were used for all NMR experiments.

Dynamic NMR experiments were performed with samples thermostated by means of a stream of liquid nitrogen vapors heated to required temperatures using a temperature controller. Because of the difficulty of ejecting the sample from the magnet at lower temperatures, the temperature calibrations were performed separately using methanol standard[27] operated at identical conditions. The uncertainties in temperature measurements are estimated to be ±1 °C. For practical reasons, most of low-temperature spectra were recorded with *rac*-**1** rather than with **1**. No differences between the spectra of the two samples were observed. Rate constants were derived from the spectra by a full line-shape analysis using gNMR ver. 3.6.5 software.[28] Standard deviations of the activation parameters were calculated talking the temperature uncertainty into account.

Force-field calculations were performed with MacroModel ver. 6.5[29] using Amber* (a MacroModel implementation of the original Amber[30]) or MMFF[31] force fields. Conformational searches were performed exhaustively using the pseudo-systematic Monte Carlo method[32] implemented in MacroModel. Energy profiles for side chain rotations were computed using the dihedral driver option in MacroModel, with full geometry optimization at each point. The rotation is to some extent coupled to the orientation of the carboxylate moiety. To avoid discontinuities in the energy profiles, the carboxylate orientation was sampled at each point. Nitrogen inversion was investigated using two-dimensional dihedral driver calculations varying the N(4)−C(5)−C(6)−C(7) backbone torsion and the C(5)−N(4)-C(3)−C(21) bridgehead improper torsion simultaneously, both in increments of 10°. For all dynamic processes, true transition states were located by constrained steepest descent optimization followed by full-matrix Newton-Raphson optimization without line searching. Gas-phase transition states were verified by normal-mode analysis. The eigenmode corresponding to the negative eigenvalue for each transition state was generated and inspected visually with the Movie facility in MacroModel. All geometries (both ground and transition states) were also subjected to reoptimization in $CHCl_3$ employing the GB/SA solvation model[33] in conjunction with the Amber* force field. Geometries were in all cases very similar to their gas-phase counterparts, and energies varied only slightly. Solvated transition states were verified by slight distortions followed by energy minimization to the flanking ground states.

Density-functional theory calculations were performed in vacuo using the B3LYP hybrid functionals[34,35] and the 6-31G* basis set in Jaguar 4.0,[36] employing default settings throughout.

Acknowledgment. We thank Dr. I. Toth, School of Pharmacy, University of Queensland, Australia, for a sample of *rac*-**1**.

JO000987N

(27) Van Geet, A. L. *Anal. Chem*. **1970**, *42*, 679.
(28) Budzelaar, P. M. H. gNMR ver. 3.6.5. Cherwell Scientific Publishing Limited, Oxford Science Park, Oxford, 1995.
(29) Weiner, S. J.; Kollman, P. A.; Nguyen, D. T.; Case, D. A. *J. Comput. Chem*. **1986**, *7*, 230.
(30) Halgren, T. A. *J. Comput. Chem*. **1996**, *17*, 490.
(31) Mohamadi, F.; Richards, N. G. J.; Guida, W. C.; Liskamp, R.; Lipton, M.; Caufield, C.; Chang, G.; Hendrickson, T.; Still, W. C. *J. Comput. Chem*. **1990**, *11*, 440.
(32) Goodman, J. M.; Still, W. C. *J. Comput. Chem*. **1991**, *12*, 1110.
(33) Still, W. C.; Tempczyk, A.; Hawley, R. C.; Hendrickson, T. *J. Am. Chem. Soc.* **1990**, *112*, 6127.
(34) Becke, A. D. *J. Chem. Phys.* **1993**, *98*, 5648.
(35) Lee, C.; Yang, W.; Parr, R. G. *Phys. Rev. B* **1988**, *37*, 785.
(36) Jaguar 4.0, Schrödinger, Inc., Portland, Oregon, 2000.